Articles

Differential Binding Modes of Diacylglycerol (DAG) and DAG Lactones to Protein Kinase C (PK-C)

Dina M. Sigano,[†] Megan L. Peach,[†] Kassoum Nacro,[†,‡] Yongseok Choi,[†] Nancy E. Lewin,[§] Marc C. Nicklaus,[†] Peter M. Blumberg,[§] and Victor E. Marquez*[,†]

Laboratory of Medicinal Chemistry, Center for Cancer Research, National Cancer Institute at Frederick, National Institutes of Health, Frederick, Maryland 21702, and Laboratory of Cellular Carcinogenesis & Tumor Promotion, Center for Cancer Research, National Cancer Institute, National Institutes of Health, Bethesda, Maryland 20892

Received October 24, 2002

Diacylglycerol lactones (DAG lactones), analogous to highly potent diacylglycerols (DAGs) were synthesized to demonstrate the ability of PK-C to discriminate between two differential binding modes, *sn*-1 and *sn*-2. While both *sn*-1 and *sn*-2 binding modes are allowable in terms of hydrogen bonding, it has been found that in general, DAGs prefer to bind *sn*-1, while the corresponding analogous DAG lactones prefer to bind *sn*-2. However, this binding orientation can be directly influenced by the disposition and nature of the acyl substituent, particularly if it is highly branched. When the "binding driving force" (i.e., the larger branched acyl chain) is in the *sn*-2 position, a dramatic increase in binding affinity is observed in the DAG lactone as compared to its open chain DAG counterpart. As these analogous DAGs and DAG lactones have almost identical log *P* values, this difference in binding affinity is a direct result of the entropic advantage of constraining the glycerol backbone.

Introduction and Background

Protein kinase C (PK-C) is a family of serine/threonine specific isozymes that are regulated by phosphorylation, by calcium, and by association with phospholipids and 1,2-diacylglycerol (DAG).[1−4] Its discovery[5] in the early 1980s as "the receptor" for the tumor-promoting phorbol esters led to a barrage of studies revealing the central role of PK-C in cell signaling. The PK-C family comprises 10 isozymes grouped into three classes: conventional (α, *β*, *γ*), novel (*δ*, *ϵ*, *η*, *θ*), and atypical (*ζ*, *ι*/*λ*). In addition, PK-C *μ* and *ν* are considered by some to constitute a fourth class and by others to comprise a distinct family called protein kinase D.[6] All members contain a C-terminal kinase domain with serine/threonine specific kinase activity and an N-terminal regulatory domain. The regulatory domain contains two key functionalities: an autoinhibitory sequence and one or two membrane-targeting domains (C1 and C2).

The accepted dogma has been that these isozymes are cytosolic in the inactive state and, as part of the activation process, translocate to the inner leaflet of the cellular membrane.[7,8] Classical (α, *β*, and *γ*) as well as novel (*δ*, *ϵ*, *η*, *θ*) PK-C isozymes become activated as a result of the association of the cytosolic enzyme with membranes containing acid phospholipids.[9,10] This association is strongly facilitated by the lipophilic second messenger, DAG, which is generated as a result of a stimulus-initiated activation of phospholipase C.[11] The binding of PK-C to the plasma membrane is transient and regulated by the association of its C1 domain with DAG in the membrane.[12]

The classical and novel PK-C isozymes each contain two small (∼50 residues) zinc fingerlike domains (C1a and C1b), consisting of two *β*-sheets and a small α-helix. The crystal structure of an isolated C1 domain from PK-C*δ* in complex with phorbol-13-O-acetate[13] showed that when the ligand is bound in the pocket between the *β*-sheets, a continuous hydrophobic surface is created over the top third of the domain, which in turn promotes its insertion into the membrane.

Previously, we have found that DAGs containing branched acyl groups exhibit a high affinity for PK-C with the presence of these branched acyl groups being of critical importance to reach binding affinities in the nanomolar range.[14] This affinity is found to be partially based on a lipophilic requirement, measured as log *P* (the octanol−water partition coefficient), provided by the acyl groups. While the absolute log *P* value cannot be used to predict binding affinity, it can be used to compare the relative lipophilicity of a compound and, therefore, to describe its degree of hydrophobic and hydrophilic binding. Aside from this receptor interaction, log *P* values are also important for membrane permeability and disposition before the drug even reaches the receptor. For binding to PK-C, optimal compounds provide hydrophobic contacts that bind to a group of conserved hydrophobic amino acids located

* To whom correspondence should be addressed. Tel: 301-846-5954. Fax: 301-846-6033. E-mail: marquezv@mail.nih.gov.
[†] Laboratory of Medicinal Chemistry, Center for Cancer Research.
[‡] Current address: Albany Molecular Research Inc., P.O. Box 15098, Albany, NY 12212.
[§] Laboratory of Cellular Carcinogenesis & Tumor Promotion, Center for Cancer Research.

10.1021/jm020476o
Published on Web 03/29/2003

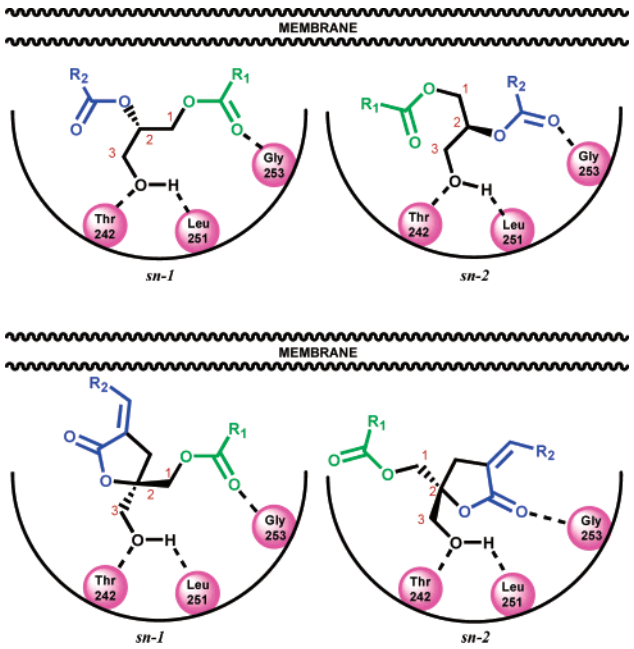

Figure 1. Hydrogen-bonding interaction of DAG (top) and DAG lactone (bottom) at the C1 domain of PK-C in the alternative binding modes of *sn*-1 (left) and *sn*-2 (right). Numbering of the PK-C residues is internal to the C1 domain (e.g., Gly 23 corresponds to Gly 253 in PK-Cδ C1b, Gly 59 in PK-Cα C1a, and Gly 124 in PK-Cα C1b). Numbering of the DAG carbon backbone is shown in red.

around the rim of the binding pocket at the top of the C1 domain where phorbol esters bind.

Docking studies using the crystal coordinates of the C1b domain of PK-Cδ in complex with phorbol-13-O-acetate[13] revealed two possible binding modes, *sn*-1 and *sn*-2, when DAG or DAG lactone[15] was docked into the empty C1b domain. Although the carbonyl moieties are not equivalent, they are able to display a similar network of hydrogen bonds to Thr12, Leu21, and Gly23—matching those seen with phorbol-13-O-acetate—in two distinct orientations with participation from the primary OH and only one of the carbonyl groups. The *sn*-1 binding mode in either DAG or DAG lactone is defined as that in which the *sn*-1 carbonyl is directly bound to the protein; while the *sn*-2 binding mode is defined as that in which the *sn*-2 carbonyl is directly bound to the protein (Figure 1).

Previously, we successfully undertook the task of identifying a DAG candidate with the lowest log *P* value that did not compromise binding affinity.[16] In doing so, nonspecific binding interactions between the DAG and the membrane were minimized and the differences in K_i values reflected changes in specific interactions between the ligand and the protein. Included in this series is **1**, the most potent, hydrophilic DAG ligand known to date. It is 1.5 log units less lipophilic than 1,2-dioctanoyl-*sn*-glycerol (diC8), activates PK-Ca ca. 2-fold better than diC8, and is capable of translocating the full-length protein efficiently to the membrane.[16] From this study, the significance of hydrophobic interactions between ligand, receptor, and phospholipid in the ternary complex has become more evident. The observed differences in the binding affinities within this DAG series were attributed to the particular orientation of the large and small branched acyl groups and their ability to interact with specific hydrophobic amino acids in the C1 domain. Thus, the contrast in K_i values between **1** and its transposed analogue (**2**) reflects the ability of PK-C to discriminate between the different orientations of the two acyl branches.

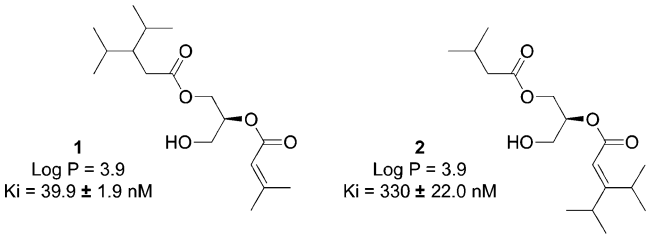

We have also observed highly potent PK-C ligands based on the DAG structure where the glycerol backbone is constrained into a five member lactone ring (DAG lactone).[14] It was discovered that the *Z* isomer of the DAG lactone **3** exhibited a 10-fold increase in binding affinity when compared to its open chain counterparts (**4** and **5**). Because these compounds, **3**−**5**, have almost identical log *P* values, this 10-fold increase in potency is believed to be the direct result of the entropic advantage of constraining the glycerol backbone.

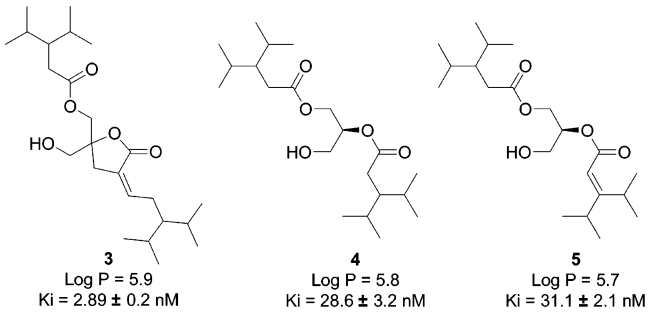

Results and Discussion

SAR Design. An exercise similar to the one described above using the corresponding DAG lactones derived from these more recently discovered,[16] less lipophilic DAGs was expected to be equally informative. DAG lactones (**6**−**9**), conceptually generated by *sn*-2 lactonization of the DAG analogues (**1** and **2**), were selected as targets to study the effect of acyl group predilection on a constrained glycerol backbone (Scheme 1). It should also be noted that despite the extra carbon required to form the lactone ring, the DAG lactones are less lipophilic than their open chain counterparts. Therefore, to keep the lipophilicity consistent between the DAGs and the DAG lactones, additional carbons were added to the *sn*-2 acyl group to increase the log *P* closer to the value of 3.9 calculated for the DAGs.

Synthesis. Lactones **6**, **7**, and **9** were synthesized according to previously published procedures.[15,17] Aldol condensation of lactone **10**[18] with acetone gave **11**, which was not isolated but directly subjected to elimination conditions to give **12**. Deprotection followed by monoacylation gave **6** (Scheme 2). Alternatively, condensation of **10** with the desired aldehyde gave a mixture of diastereomeric alcohols, which were not isolated but immediately subjected to elimination conditions. A mixture of *E* and *Z* olefin isomers (**16** and **17**) was obtained in ca. 2:1 ratio and was readily separated by

Scheme 1

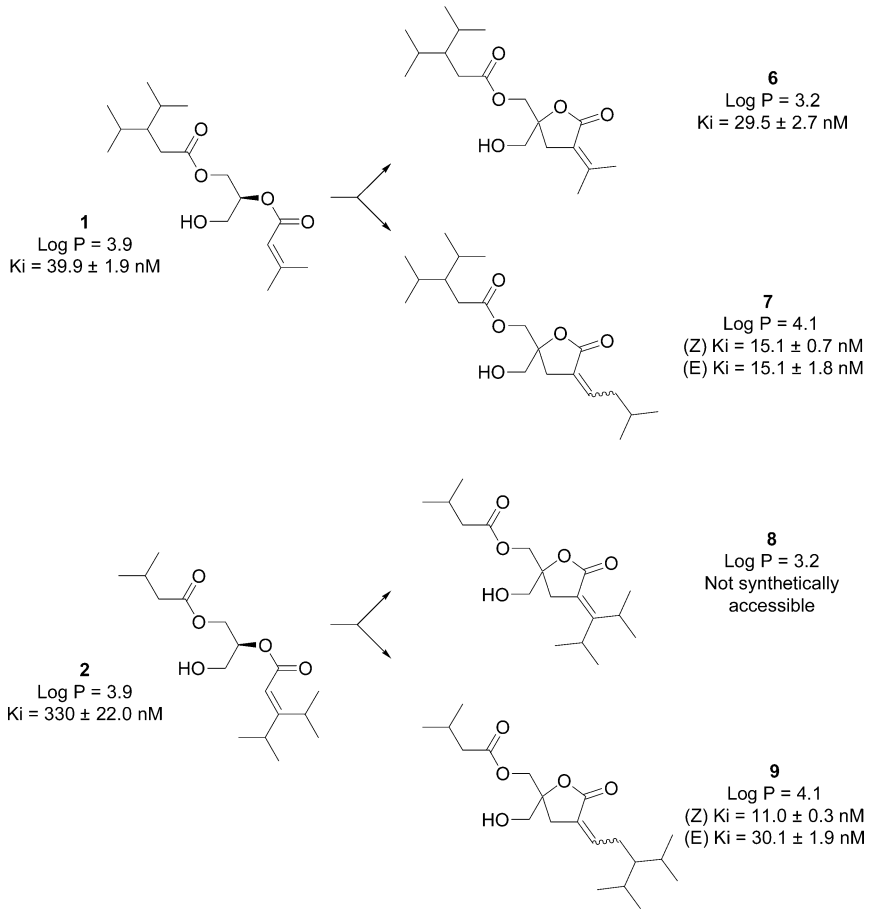

Scheme 2

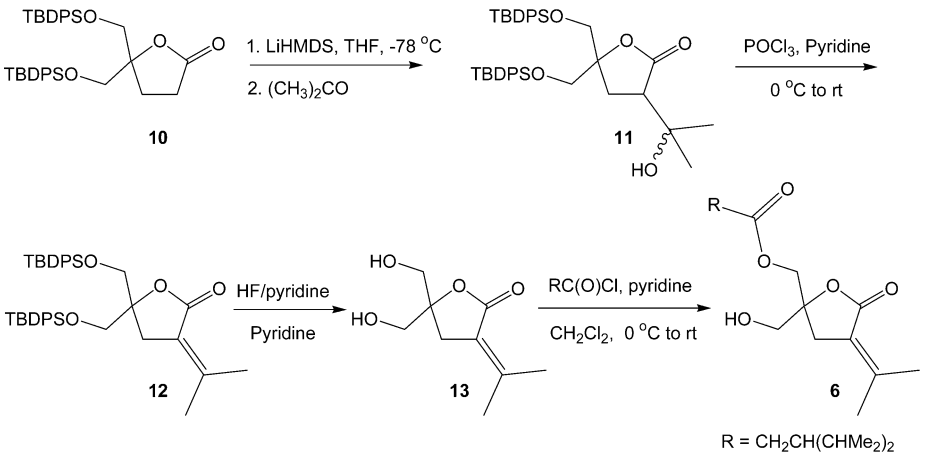

column chromatography. Deprotection followed by monoacylation gave the desired DAG lactones, **7** and **9** (Scheme 3).

Biological Activity. Binding affinity assays were done with intact recombinant PK-Cα, an isozyme where both the C1a and the C1b domains are involved in ligand binding and membrane translocation.[19] The interaction of the DAGs and DAG lactones was assessed in terms of the ability of the ligand to displace bound [20-^{3}H]phorbol-12,13-dibutyrate (PDBu) in the presence of phosphatidylserine. The inhibition curves obtained for all ligands were of the type expected for competitive inhibition, and the ID_{50} values were determined by fit of the data points to the theoretical noncooperative competition curve. The K_i values for inhibition of binding were calculated from the ID_{50} values. The octanol/water partition coefficients (log *P*) were calculated according to the fragment-based program KOWWIN 1.63[20] (Scheme 1).

Interestingly, DAG lactones **6** and **7**, analogues of the most potent DAG (**1**), did not show the expected 10-fold increase in binding. In fact, while the K_i values of lactones **6** and **7**, with the larger acyl branch at the *sn*-1 position, were slightly lower, they were within a factor $\leq$2.5 of that for DAG **1**. While DAG lactone **8** was not synthetically accessible, when we compared DAG lactone **9**, derived from DAG **2**, with the larger acyl branch at the *sn*-2 position, we saw a dramatic increase in

Scheme 3

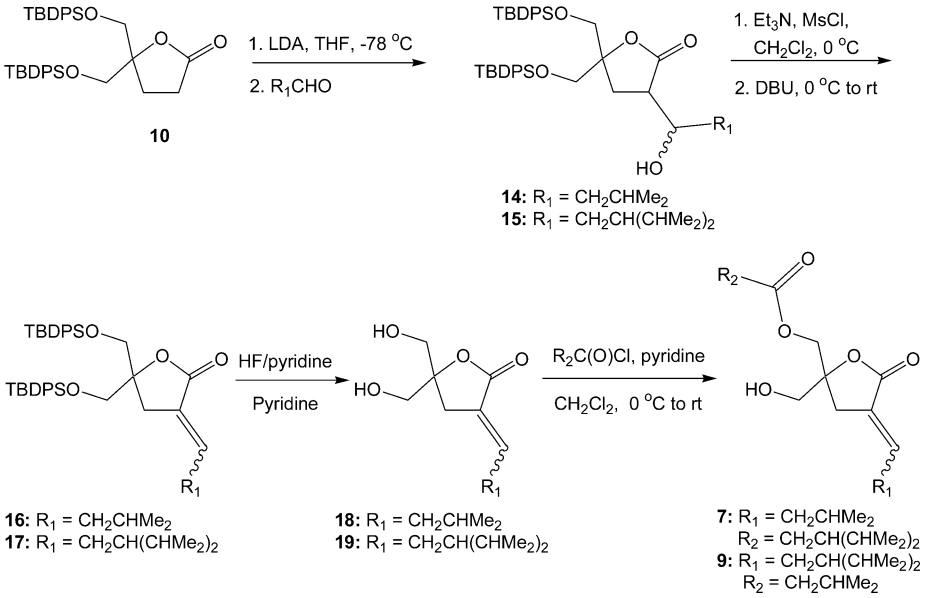

binding. Indeed, the more potent *Z* isomer, **9***Z*, showed a 33-fold increase in binding when compared to **2**. Even the less potent *E* isomer (**9***E*) exhibited 10-fold better binding. It is also worth noting that for the sake of synthetic expediency, the DAG lactones synthesized are racemic; hence, the potency for all known active (*R*)-DAG lactone enantiomers should be approximately doubled.[21]

Molecular Modeling. For computational docking studies, homology models of the C1a and C1b domains of PK-Cα were built based on the crystal structure of the C1b domain of PK-Cδ.[13] The open chain DAGs **1** and **2**, along with the *E* and *Z* isomers of the corresponding DAG lactones **7** and **9**, which have comparable log *P* values, were docked into both the C1a and the C1b domains using the docking programs FlexX[22] and GOLD.[23]

Surprisingly, the docking results from FlexX and GOLD were not consistent. FlexX docked the DAG ligands exclusively in only one of the two possible orientations—*sn*-1 for the open chain DAGs and *sn*-2 for DAG lactones. GOLD, however, produced a mixture of *sn*-1 and *sn*-2 orientations in all cases, in a manner similar to previous docking studies with DAG ligands using the program AutoDock.[15,16,24] In some cases, the highest ranked GOLD structure of a DAG lactone was docked *sn*-1, but all of the FlexX structures were docked in the *sn*-2 orientation for all of the DAG lactones. Therefore, in an attempt to determine which orientation is preferred, the docked *sn*-1 and *sn*-2 structures for all of the DAG ligands were analyzed in further detail.

The highest scoring conformation of each ligand docked in a specific orientation into either the C1a or the C1b receptor was selected and refined with 100 cycles of simulated annealing to generate an ensemble of similar low-energy structures for each docked conformation, and the average hydrogen-bonding interaction energy between PK-C and DAG for each ensemble was calculated (Table 1). Because small changes in receptor−ligand conformation can produce very large differences in electrostatic energy, averaging over an ensemble smoothes out any spurious energy differences and allows more accurate analysis and comparison of the relative energies of the two binding modes for each ligand.

Table 1. Hydrogen-Bonding Interaction Energies (kcal/mol) and Buried Surface Areas (Å^2) between DAG Ligands and the C1 Domains of PK-Cα

	H-bonding energy		buried surface area	
	C1a	C1b	C1a	C1b
DAG **1** bound *sn*-1	−120.33	−115.30	547.59	563.74
DAG **1** bound *sn*-2	−61.22	−102.35	533.31	547.11
DAG **2** bound *sn*-1	−119.59	−107.60	548.92	555.47
DAG **2** bound *sn*-2	−87.52	−100.52	553.62	562.27
DAG lactone **7Z** bound *sn*-1	−61.21	−88.76	554.71	572.41
DAG lactone **7Z** bound *sn*-2	−97.49	−147.27	511.66	558.38
DAG lactone **7E** bound *sn*-1	−53.34	−83.51	567.01	542.95
DAG lactone **7E** bound *sn*-2	−94.84	−145.13	540.79	532.20
DAG lactone **9Z** bound *sn*-1	−57.19	−83.88	514.20	523.70
DAG lactone **9Z** bound *sn*-2	−123.80	−175.14	520.91	618.23
DAG lactone **9E** bound *sn*-1	−53.37	−82.08	559.36	522.83
DAG lactone **9E** bound *sn*-2	−80.49	−143.06	501.62	536.45

For each ensemble, the average difference in solvent accessible surface area between the bound complex and the unbound ligand and receptor was also calculated (Table 1). This number is related to the nonpolar component of the solvation energy (i.e., the hydrophobic effect). Thus, the size of the surface area that is buried upon ligand binding is a good measure of the strength of the hydrophobic interactions between ligand and receptor.

For the open chain DAGs (**1** and **2**), in both the C1a and the C1b domains of PK-Cα, the hydrogen-bonding energy is stronger (lower) with *sn*-1 binding (Table 1). This agrees with our previous study,[16] where we observed shorter hydrogen-bonding distances in the *sn*-1 orientation for a series of DAG compounds. When the larger acyl side chain is next to the *sn*-1 carbonyl, as in DAG **1**, the size of the buried surface area upon ligand binding is also larger with *sn*-1 binding, suggesting that this compound favors the *sn*-1 orientation (Table 1). However, when the larger acyl side chain is next to the *sn*-2 carbonyl, as in DAG **2**, although the hydrogen-binding energy is stronger with *sn*-1 binding, the size of the buried surface area is larger with *sn*-2 binding.

This antagonism of forces is mirrored with the DAG lactones **7** and **9**. Hydrogen bonding for the lactones is stronger in the *sn*-2 orientation (Table 1), and this binding mode is reinforced by the increased size of the buried surface area when the bulkier side chain is next to the binding (*sn*-2) carbonyl as in **9***Z*. For **7***E* and **7***Z* however, although the hydrogen bonding is stronger for the *sn*-2 orientation, the buried surface area is increased in the *sn*-1 orientation due to the bulkier side chain being on the *sn*-1 carbonyl.

For the DAG ligands **1** and **9***Z*, the modeling results unequivocally show which binding mode is more favorable, whereas for the ligands **2** and **7***E*/*Z*, deducing the correct binding mode depends on whether binding is driven more by hydrogen-bonding interactions or by hydrophobic interactions between receptor and ligand. The hydrophobic effect is generally considered to be the major driving force for protein folding and is likely also to be the driving force for interactions between PK-C and its DAG ligands, especially since it is the formation of a continuous hydrophobic surface over the top of the bound complex that drives membrane translocation and activation of PK-C. This suggests that DAG **2** will bind in the *sn*-2 orientation to maximize its hydrophobic interactions with PK-C, whereas the DAG lactones **7***E*/*Z* will probably bind in the *sn*-1 orientation for these same reasons.

These results also give an explanation for the discrepancy between the docking results from FlexX and those from GOLD. The docking algorithm in FlexX begins by placing a core fragment into the binding site, and then, the rest of the ligand is built up piece by piece. Because hydrogen-bonding interactions are stronger in the *sn*-1 orientation for the open chain DAGs and stronger in the *sn*-2 orientation for the DAG lactones, this determines the orientation in which FlexX will always place the core fragment. GOLD, on the other hand, uses a genetic algorithm to place the whole ligand in the binding site at once, and its internal scoring function is weighted to favor hydrophobic van der Waals interactions, thus giving a mixture of *sn*-1 and *sn*-2 binding.

Some interesting patterns that differentiate the mode of binding between DAGs and their corresponding lactones have begun to emerge. The open chain DAGs appear to prefer to bind in the *sn*-1 mode.[16] This binding mode can be reinforced by the presence of a highly branched alkyl chain next to this carbonyl, such as in **1**. However, the disposition of the branched alkyl chains can alter this preference and force the less efficient *sn*-2 binding mode, resulting in a weaker ligand, such as **2**. From the present work, we learn that the situation with the DAG lactones seems to be the reverse. It appears that the *sn*-2 binding mode is favored for the DAG lactones (**6**−**9**) and this reversed binding mode hypothesis is confirmed by the binding results. We observe that lactonization of the most efficient DAG leads to a less efficient DAG lactone, while the less efficient DAG leads to a more efficient DAG lactone. Here, too, the location of the branched alkyl chain drives the binding mode. If the branched alkyl chain is adjacent to the *sn*-1 carbonyl, the DAG lactone binds such as a DAG (*sn*-1) and no entropic benefit is derived from the cyclization. However, if the location of the branched alkyl chain is adjacent to the lactone carbonyl engaged in binding (i.e., *sn*-2), the binding affinity increases at least ca. 10-fold and is also sensitive to the *E* and *Z* stereochemistry of the double bond as the presence of the α,*β*-unsaturated system in the lactones creates restricted rotation near the Gly23 binding site.

A surface representation of the empty binding site shown from above (Figure 2A) offers a structural explanation for the importance of the disposition of the larger branched acyl chain. In the center of the binding pocket is a deep cavity, where the primary OH group binds to the backbones of Thr12 and Leu21.[25] The rim of the binding site is lined with hydrophobic residues and contains three "pockets" through which the acyl chains of DAG and other ligands can extend into the membrane. One small, shallow pocket is located between Pro11 and Leu20; a second, medium-sized pocket is located between Gly9 and Leu24; and the third, largest pocket is located between Leu20 and Leu24, across Gly23. This glycine residue at position 23 is absolutely conserved across all C1 domains in the PK-C isozyme family, suggesting that it is vital to the structure and function of these domains.

When the larger acyl chain is next to the carbonyl that binds to Gly23, as in the *sn*-1 orientation of DAG **1** (Figure 2B) or the *sn*-2 orientation of DAG lactone **9***Z* (Figure 2E), the ligand fits neatly into the large pocket between Leu20 and Leu24. The acyl chain of the ligand is buried, and the gap in the hydrophobic surface of the receptor is filled. However, when the smaller acyl chain is next to the binding carbonyl, as in the *sn*-2 orientation of DAG **1** (Figure 2C) or the *sn*-1 orientation of DAG lactone **9***Z* (Figure 2F), it is not sufficiently large to fill this large pocket. In this orientation, the bulkier acyl chain is forced into the smaller gap between Gly9 and Leu24, where it is not completely buried.

DAG lactone **9***E*, on the other hand (Figure 2D), cannot conform to the geometry of the binding site due to restricted rotation about the double bond. When binding in the *sn*-2 orientation, the bulkier acyl chain packs into the small, shallow pocket near Pro11, instead of fitting into the pocket between Leu20 and Leu24. This isomer may in turn prefer to bind in the less efficient *sn*-1 mode, which explains its lower binding affinity relative to the *Z* isomer (Table 1).

DAG lactones **7***E* and **7***Z*, derived from the lactonization of **1**, most likely bind *sn*-1. This mode of binding in DAG lactones appears to be driven by the presence of the bulkier branched chain on this carbonyl. Because there is no restricted rotation of the branched alkyl chain in the environment of the *sn*-1 carbonyl, there is no difference in the binding between *E* and *Z* isomers; because the carbonyl involved in binding (*sn*-1) is not a component of the lactone ring, there is not a significant entropic advantage (<3-fold in the best case) due to lactonization.

However, DAG lactone **9***Z*, derived from the lactonization of **2**, most likely binds *sn*-2, and because the carbonyl engaged in binding is the lactone carbonyl, a ca. 10-fold increase in binding affinity is seen relative to its parent DAG. Here, too, the binding mode appears to be driven by the bulkier side chain now adjacent to the lactone carbonyl. Because the lactone (*sn*-2) carbonyl is the one engaged in binding, we observe a 2−3-fold

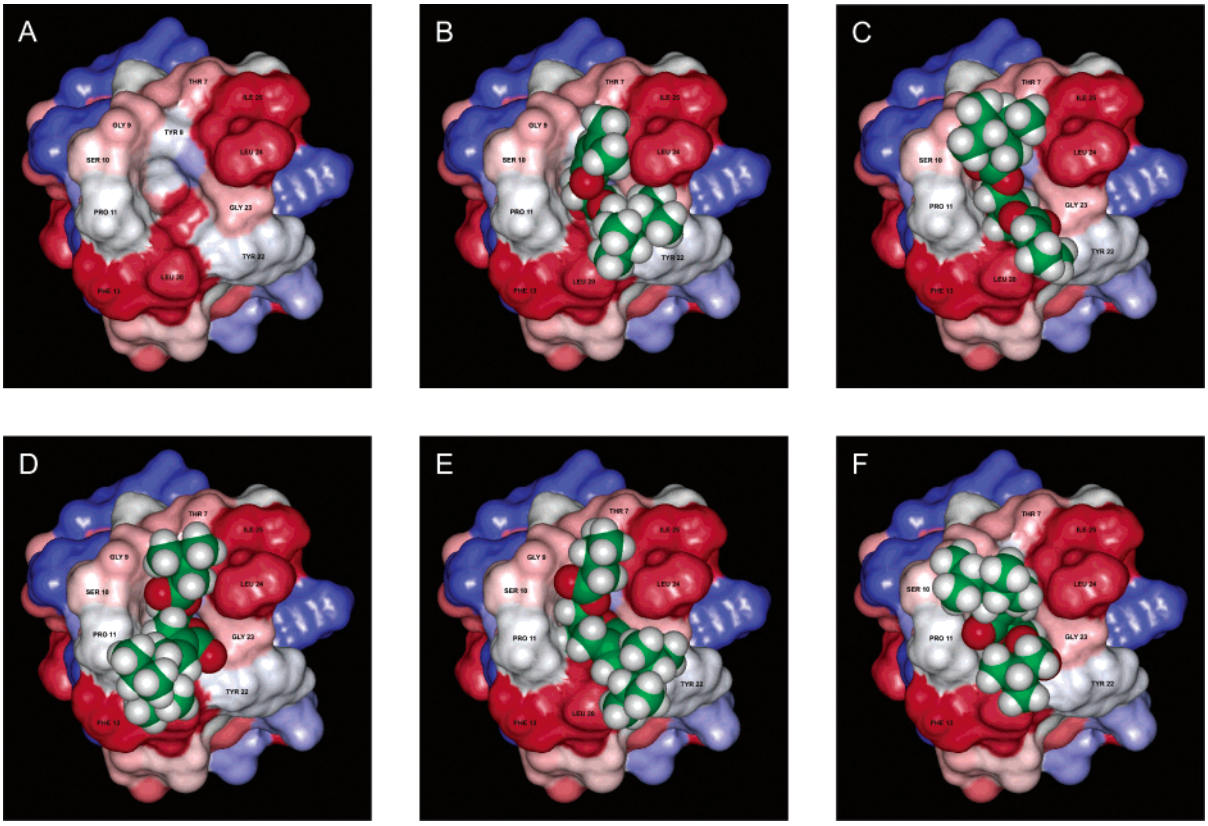

Figure 2. (A) Empty C1B domain of PK-Cα; (B) DAG **1** bound *sn*-1; (C) DAG **1** bound *sn-2*; (D) E-DAG lactone **9** bound *sn-2*; (E) Z-DAG lactone **9** bound *sn*-2; (F) Z-DAG lactone **9** bound *sn*-1. The DAG ligands are shown in CPK representation and colored by atom type (C = green; H = white; O = red). The Connolly surface of the receptor was generated using Insight II (2000) and is colored by residue hydrophobicity (blue = hydrophilic; red = hydrophobic). Residue numbering is internal to the C1 domain.

difference between the *Z* and the *E* isomers due to the restricted rotation of the alkyl chain in the environment of this carbonyl and its effect on the interaction with the C1 domain. This result suggests that such an interaction is with the C1 domain and not with the lipid where the stereochemical disposition of the alkyl chain would be expected to be less important.

Observations and Conclusions

The ability of PK-C to discriminate between the different orientations of the acyl branches is clearly demonstrated by this study. We observe that in terms of hydrogen bonding, both *sn*-1 and *sn*-2 binding modes are allowed. In general, the open chain DAGs prefer to bind *sn*-1, while the corresponding DAG lactones prefer to bind *sn*-2. However, the disposition and nature of the acyl chain, particularly if it is highly branched, can have a direct influence on the binding orientation. When the "binding driving force" (i.e., the larger branched acyl chain) is in the *sn*-2 position, a dramatic increase in binding affinity is observed in the DAG lactone as compared to its open chain DAG counterpart. As these analogous DAGs and DAG lactones have almost identical log *P* values, this difference in binding affinity is a direct result of the entropic advantage of constraining the glycerol backbone.

Experimental Section

Computational Modeling. Homology Modeling. Homology models of the C1a and C1b domains of PK-Cα were built on the backbone coordinates of the crystal structure of the C1b domain of PK-Cδ.[13] The sequences of PK-Cδ C1a and PK-Cα C1b are 42% identical and 54% similar, those of PK-Cδ C1b and PK-Cα C1b are 62% identical and 80% similar, and the zinc-binding residues and residues essential for ligand binding are highly conserved. This suggests that the backbone structure will be very similar for all three C1 domains. Side chains for the homology models were constructed using the program SCWRL,[27] which uses a backbone-dependent rotamer library to place residues in their most likely conformation given the backbone $\phi-\psi$ angles at that position. Residues homologous to PK-Cδ were left unchanged from their crystallographic positions. The homology models were refined with a small energy minimization, with phorbol-13-O-acetate left in position from the crystal structure to prevent the binding site loops from closing during the minimization. Harmonic positional restraints on the backbone atoms were gradually relaxed over the course of the minimization to eliminate steric clashes in the side chains without inducing deformations in the backbone.

Docking. FlexX was run through its SYBYL module,[28] with default options throughout. The binding site was defined as residues 8−13, 20−24, and 27. Standard default settings were also used in GOLD, with the binding site defined by atoms within a 10.0 Å radius of the Nϵ atom of residue Q27. To overcome GOLD's tendency to dock the DAG ligands with one hydrophobic chain buried in the binding site, a template similarity constraint was added to the hydrogen bond acceptor atoms in the crystal structure of bound phorbol-13-O-acetate.

Refinement. The highest scoring structure for the *sn*-1 and *sn*-2 conformations of each ligand in each C1 domain (from either the FlexX or the GOLD results) was selected for further refinement. All simulations were run in CHARMM[29] version 28n1 or 27b3, and the all atom CHARMM 22 force field,[30] which includes parameters for general organic compounds as well as amino acids, was used. Missing parameters and partial charges for the DAG ligands were generated in QUANTA 97.[27] No explicit waters were included, and the nonbonded interactions were calculated without cutoffs and with a constant

dielectric of 1.0 to mimic the low-dielectric environment of the membrane. Only the binding site residues (7−13, 20−24, and 27) were free to move along with the ligand; all other residues were held fixed. Gentle constraints holding the distance between the atoms involved in the three hydrogen bonds between the DAG ligand and the protein (Figure 1) at less than 3.0 Å were included to keep the ligand in the binding site during high-temperature molecular dynamics and to preserve its *sn*-1 or *sn*-2 orientation. The docked structures were first minimized with the Adopted Basis Newton−Raphson algorithm until the RMS value of the derivatives reached a convergence of 0.001, then heated in 10° increments every 200 steps from a starting temperature of 50−300 K, and equilibrated at 300 K for 10 000 steps. During equilibration, the atomic velocities were reassigned according to a random Gaussian distribution every 200 steps. Simulated annealing was performed by rapidly heating the system from 300 to 500 K at a rate of 1° per step, maintaining it at 500 K for 500 steps, and then slowly cooling by 5° every 100 steps back to 300 K. This cycle was repeated 100 times, and the structure at the endpoint of each cycle was minimized to convergence as before to yield an ensemble of 100 low-energy structures for each docked conformation.

Analysis. The hydrogen-bonding energy for each structure was calculated in CHARMM by first defining four atom subsets consisting of ligand donor atoms, ligand acceptor atoms, receptor donor atoms, and receptor acceptor atoms. Each potential donor−acceptor pair was tested to see whether it was within allowable hydrogen-bonding geometry (i.e., with an H···A distance of 2.7 Å or less and a D−H···A angle greater than 90°). If so, the nonbonded (electrostatic and van der Waals) interaction energy between the two atoms was calculated. The sum total of these interaction energies for all of the structures in the ensemble was then divided by 100 to give the average hydrogen-bonding energy for the ensemble. The solvent accessible surface areas (SASA) for the ligand alone, the receptor alone, and the bound complex were also computed in CHARMM, using the Lee and Richards algorithm,[31] a probe radius of 1.4 Å, and van der Waals radii for all atoms. The size of the buried surface area upon ligand binding was calculated as the SASA of the bound complex subtracted from the sum of the SASA of the unbound receptor and ligand. The average buried surface area was calculated for each ensemble.

1-(3-Isopropyl-4-methylpentanoyl)-2-(3-methylbut-2-enoyl)-*sn*-glycerol (1). This compound has been previously reported.[16]

1-(3-Methylbutanoyl)-2-(3-isopropyl-4-methylpent-2-enoyl)-*sn*-glycerol (2). This compound has been previously reported.[16]

(*Z*)-{2-(Hydroxymethyl)-4-[4-methyl-3-(methylethyl)-pentylidene]-5-oxo-2-2,3-dihydrofuryl}methyl-4-methyl-3-(methylethyl)pentanoate (3). This compound has been previously reported.[14]

1,2-Di-(3-isopropyl-4-methylpentanoyl)-*sn*-glycerol (4). This compound has been previously reported.[16]

1-(3-Isopropyl-4-methylpentanoyl)-2-(3-isopropyl-4-methylpent-2-enoyl)-*sn*-glycerol (5). This compound has been previously reported.[16]

5,5-Bis[(2,2-dimethyl-1,1-diphenyl-1-silapropoxy)methyl]-3,4,5-trihydrofuran-2-one (10). This compound has been previously reported.[18]

5,5-Bis[(2,2-dimethyl-1,1-diphenyl-1-silapropoxy)methyl]-3-(1-hydroxy-isopropyl)-3,4,5-trihydrofuran-2-one (11). Under argon, LiHMDS (3.5 mL, 1 M solution) was added dropwise to a −78 °C solution containing **10** (2.0 g, 3.2 mmol) in THF (8 mL) and stirred at −78 °C for 1 h, after which acetone (250 μL, 3.5 mmol) was added slowly. After 21 min, the reaction was diluted with Et_2O (25 mL) and quenched with saturated aqueous NH_4Cl. The phases were separated, and the aqueous phase was extracted with Et_2O (3 × 25 mL). The combined organic phases were dried over $MgSO_4$ and concentrated to give **11**, which was used directly without further purification.

5,5-Bis[(2,2-dimethyl-1,1-diphenyl-1-silapropoxy)methyl]-3-(methylethylidene)-4,5-dihydrofuran-2one (12). $POCl_3$ was added dropwise to a 0 °C solution of **11** in pyridine (15 mL), which was allowed to reach room temperature overnight. The reaction was diluted with Et_2O, washed with 10% aqueous $CuSO_4$ solution (3×), dried over Na_2SO_4, and concentrated. Isolation by silica gel chromatography gave **12** (2.07 g, 97% from **10**), which was used without further purification. ^{1}H NMR (300 MHz, $CDCl_3$): δ 1.08 (s, 18 H, CH_2-OSiPh_2tBu), 1.92 (s, 3 H, C=CHMe_2), 2.34 (s, 3 H, C=CHMe_2), 2.82 (s, 2 H, lactone-CH_2), 3.78−3.80 (m, 4 H, CH_2OSiPh_2tBu), 7.41−7.51 (m, 12 H, SiPh_2tBu), 7.71−7.68 (m, 8 H, OSiPh_2tBu). ^{13}C NMR (75 MHz, $CDCl_3$): δ 19.18, 19.70, 24.33, 32.33, 66.37, 83.14, 127.62, 132.66, 132.84, 135.49, 148.26, 169.54.

General Procedure for Condensation/Dehydration for Compounds 16*E*/*Z* and 17*E*/*Z*. Under argon, LDA (1.4 equiv, 2 M solution) was added to a −78 °C solution of lactone (1 equiv) in THF (6 mL/mmol). After it was stirred at −78 °C for 2 h, a solution of aldehyde (4 equiv) in THF (6 mL/mmol) was added dropwise. The reaction was kept at −78 °C and monitored by thin-layer chromatography (TLC). After the designated time, the reaction mixture was quenched at −78 °C with aqueous NH_4Cl (6 mL/mmol), warmed to room temperature, extracted with Et_2O (3×), dried over $MgSO_4$, and concentrated in vacuo to give the hydroxy adduct, which was used without further purification.

The crude product was then dissolved in CH_2Cl_2 (7 mL/mmol) containing pyridine (4 equiv) and cooled to 0 °C. MsCl (2 equiv) was added dropwise, and the reaction was stirred at 0 °C for 30 min and then at room temperature for 90 min. The reaction mixture was then cooled again to 0 °C, DBU (5 equiv) was added dropwise, and the reaction reached room temperature overnight. The crude mixture was then filtered through a thin pad of Celite, concentrated, and purified by column chromatography to give both the *E* and the *Z* isomers.

5,5-Bis[(2,2-dimethyl-1,1-diphenyl-1-silapropoxy)methyl]-3-[1-hydroxy-4-methyl-3-(methylethyl)pent-2-enyl]-oxolan-2-one (15). This compound has been previously reported.[15]

(*Z*)-5,5-Bis[(2,2-dimethyl-1,1-diphenyl-1-silapropoxy)-methyl]-3-(3-methylbutylidene)-4,5-dihydrofuran-2-one (16*Z*). Yield: 0.806 g, 27%. IR (neat): 2957 (CH), 2870 (CH), 1759 (C=O), 1671 (C=C) cm^{-1}. ^{1}H NMR (400 MHz, $CDCl_3$): δ 0.94 (d, J = 6.6 Hz, 6 H, C=CHCH$_2$CHMe_2), 1.02 (s, 9 H, CH_2OSiPh_2tBu), 1.72 (apparent septet, J = 6.7 Hz, 1 H, C=CHCH$_2$CHMe$_2$), 2.63 (tt, J = 7.2, 2.0 Hz, 2 H, C=CHCH_2CHMe$_2$), 2.86 (m, 2 H, lactone-CH_2), 3.72 (AB quartet, J = 10.6 Hz, 4 H, CH_2SiPh$_2t$Bu), 6.14−6.19 (m, 1H, C = CHCH$_2$CHMe$_2$) 7.34−7.45 (m, 12 H, SiPh_2tBu), 7.62−7.65 (m, 8 H, SiPh_2tBu). ^{13}C NMR (100 MHz, $CDCl_3$): δ 19.21, 22.34, 26.69, 28.60, 33.10, 36.22, 65.99, 84.30, 127.74, 129.78, 132.71, 132.90, 135.57, 142.21, 169.30. FAB-MS (*m*/*z*, relative intensity): 633 (MH$^+$−C$_4$H$_{10}$, 11), 135 (100). Anal. (C$_{43}$H$_{54}$O$_4$Si$_2$) C, H.

(*E*)-5,5-Bis[(2,2-dimethyl-1,1-diphenyl-1-silapropoxy)-methyl]-3-(3-methylbutylidene)-4,5-dihydrofuran-2-one (16*E*). Yield: 1.8 g, 52%. IR (neat): 2930 (CH), 2857 (CH), 1760 (C=O), 1685 (C=C) cm^{-1}. ^{1}H NMR (400 MHz, $CDCl_3$): δ 0.98 (d, J = 6.6 Hz, 6 H, C=CHCH$_2$CHMe_2), 1.04 (s, 18 H, CH_2OSiPh_2tBu), 1.84 (apparent septet, J = 6.7 Hz, 1 H, C=CHCH$_2$CHMe$_2$), 2.06−2.10 (m, 2 H, C=CHCH_2CHMe$_2$), 2.80−2.81 (m, 2 H, lactone-CH_2), 3.75 (AB quartet, J = 10.7 Hz, 4 H, CH_2SiPh$_2t$Bu), 6.78 (tt, J = 7.6, 2.9 Hz, 1 H, C = CHCH$_2$-CHMe$_2$) 7.36−7.47 (m, 12 H, SiPh_2tBu), 7.63−7.66 (m, 8 H, SiPh_2tBu). ^{13}C NMR (100 MHz, $CDCl_3$): δ 19.17, 22.48, 26.64, 28.07, 29.73, 39.22, 66.10, 85.16, 127.74, 129.78, 132.59, 132.84, 135.53, 138.61, 170.42. FAB-MS (*m*/*z*, relative intensity): 633 (MH$^+$−C$_4$H$_{10}$, 29), 135 (100). Anal. (C$_{43}$H$_{54}$O$_4$Si$_2$) C, H.

(*Z*)-5,5-Bis[(2,2-dimethyl-1,1-diphenyl-1-silapropoxy)-methyl]-3-[4-methyl-3-(methylethyl)pentylidene)-4,5-dihydrofuran-2-one (17*Z*). This compound has been previously reported.[15]

(*E*)-5,5-Bis[(2,2-dimethyl-1,1-diphenyl-1-silapropoxy)-methyl]-3-[4-methyl-3-(methylethyl)pentylidene)-4,5-dihydrofuran-2-one (17*E*). This compound has been previously reported.[15]

General Procedure for Desilylation. Under argon, HF/pyridine (4.0 equiv, 70% solution) was added dropwise to a 0 °C stirring solution of lactone (1.0 equiv) in CH_2Cl_2 (2 mL/mmol) and the reaction was allowed to warm to room temperature overnight. The reaction was quenched by adding solid $NaHCO_3$, filtered, concentrated, and purified by column chromatography.

5,5-Bis(hydroxymethyl)-3-(methylethylidene)-4,5-dihydrofuran-2-one (13). Yield: 0.549 g, 100%, white crystals; mp 89−90 °C. IR (neat): 3379 (OH), 2882 (CH,), 2826 (CH), 1713 (C=O), 1660 (C=C) cm^{-1}. ^1H NMR (300 MHz, $CDCl_3$): δ 1.95 (s, 3 H, C=C*Me*$_2$), 2.31 (s, 3 H, C=C*Me*$_2$), 2.79 (br s, 2 H, CH_2*OH*), 3.28 (s, 2 H, lactone-C*H*$_2$), 3.78 (app q, J = 12.0 Hz, 4 H, C*H*$_2$OH). ^{13}C NMR (100 MHz, $CDCl_3$): δ 19.89, 24.52, 31.61, 64.72, 83.57, 119.47, 151.47, 170.16. FAB-MS (*m*/*z*, relative intensity): 187 (MH^+, 100). Anal. ($C_9H_4O_4$) C, H, O.

(*Z*)-Bis(hydroxymethyl)-3-(3-methylbutylidene)-4,5-dihydrofuran-2-one (18*Z*). Yield: 0.306 g, 78%. This compound was obtained as a colorless oil, which contained a small amount of the *E* isomer. Because the *E* and *Z* isomers were inseparable, the following step was carried out with this mixture.

(*E*)-Bis(hydroxymethyl)-3-(3-methylbutylidene)-4,5-dihydrofuran-2-one (18E). Yield: 0.043 g, 80%, white crystals; mp 64−65 °C. IR (neat): 3303 (OH), 2957 (CH), 2883 (CH), 1748 (C=O), 1677 (C=C) cm^{-1}. ^1H NMR (400 MHz, $CDCl_3$): δ 0.88 (d, J = 6.6 Hz, 6 H, C=CHCH$_2$CH*Me*$_2$), 1.74 (apparent septet, J = 6.7 Hz, 1 H, C=CHCH$_2$C*H*Me$_2$), 1.98−2.02 (m, 2 H, C=CHC*H*$_2$CHMe$_2$), 2.64−2.65 (m, 2 H, lactone-C*H*$_2$), 3.60 (dd, J = 12.1, 6.2 Hz, 2 H, C*H*$_2$OH), 3.69 (dd, J = 12.3, 6.1 Hz, 2 H, C*H*$_2$OH), 4.09 (t, J = 6.2 Hz, 2 H, CH$_2$O*H*), 6.62−6.67 (m, 1H, C = *CH*CH$_2$CHMe$_2$). ^{13}C NMR (100 MHz, $CDCl_3$): δ 22.36, 28.01, 29.43, 39.20, 64.65, 85.77, 127.24, 140.72, 171.15. FAB-MS (*m*/*z*, relative intensity): 215 (MH^+, 100). Anal. ($C_{11}H_{18}O_4$) C, H.

(*Z*)-5,5-Bis(hydroxymethyl)-3-[4-methyl-3-(methylethyl)pentylidene]-4,5-dihydrofuran-2-one (19*Z*). This compound has been previously reported.[15]

(*E*)-5,5-Bis(hydroxymethyl)-3-[4-methyl-3-(methylethyl)pentylidene]-4,5-dihydrofuran-2-one (19*E*). This compound has been previously reported.[15]

General Procedure for Acylation for Compounds 6 and 7*E*/*Z*. Under argon, the acid chloride (1.5 equiv) was added to a 0 °C stirring solution of lactone (1.0 equiv) and pyridine (3.0 equiv) in CH_2Cl_2 (16 mL/mmol). The reaction was monitored by TLC and then concentrated in vacuo. Purification by column chromatography gave the desired product along with a minor amount of the diacylated product.

[2-(Hydroxymethyl)-4-(methylethylidene)-5-oxo-2-2,3-dihydrofuryl]methyl-4-methyl-3-(methylethyl)pentanoate (6). Yield: 0.059 g, 56%. IR (neat): 3470 (OH), 2959 (CH), 2875 (CH), 1740 (C=O), 1666 (C=C) cm^{-1}. ^1H NMR (400 MHz, $CDCl_3$): δ 0.79 (dd, J = 6.7, 0.9 Hz, 6 H, C(O)CH$_2$CH(CH*Me*$_2$)$_2$), 0.88 (d, J = 6.8 Hz, 6 H, C(O)CH$_2$CH(CH*Me*$_2$)$_2$), 1.55 (pentet, J = 5.8 Hz, 1 H, C(O)CH$_2$*CH*(CHMe$_2$)$_2$), 1.69−1.77 (m, 2 H, C(O)CH$_2$CH(*CH*Me$_2$)$_2$), 1.86 (s, 3 H, C=C*Me*$_2$), 2.19 (d, J = 5.9 Hz, 2 H, lactone *CH*$_2$), 2.24 (app t, J = 2.2 Hz, 3 H, C=C*Me*$_2$), 2.61−2.67 (m, 2 H, C*CH*$_2$OC(O)CH$_2$CH(CHMe$_2$)$_2$ and OH), 2.79−2.85 (m, 1 H, C(O)*CH*$_2$CH(CHMe$_2$)$_2$), 3.61 (dd, J = 12.0, 4.6 Hz, 1 H, C*H*$_2$OH), 3.69 (dd, J = 11.9, 5.3 Hz, 1 H, C*H*$_2$OH), 4.18 (AB quartet, J = 11.9 Hz, 2H, C(O)-C*H*$_2$CH(CHMe$_2$)$_2$). ^{13}C NMR (100 MHz, $CDCl_3$): δ 18.66, 19.91, 21.26, 24.54, 29.33, 32.03, 32.80, 46.87, 64.85, 65.54, 81.19, 119.00, 151.54, 169.05, 174.72. FAB-MS (*m*/*z*, relative intensity): 327 (MH^+, 100). Anal. ($C_{18}H_{30}O_5 \cdot 0.25H_2O$) C, H.

(*Z*)-[2-(Hydroxymethyl)-4-(3-methylbutylidene)-5-oxo-2-2,3-dihydrofuryl]methyl-4-methyl-3-(methylethyl)pentanoate (7*Z*). According to the general procedure, 4-methyl-3-(methylethyl)pentanoyl chloride[15] was added to a solution of **18** (0.114 g, 1.6 mmol, mixture of *E* and *Z* isomers) in CH_2Cl_2 (8.6 mL) containing pyridine (129 μL) to give isolated **7*Z*** as a colorless oil (0.041 g, 22%) along with an unseparated mixture of **7*E*/*Z*** as a pale oil (0.077 g, 41%) and diacylated product (ca. 25%, not isolated). **7*Z***: IR (neat): 3465 (OH), 2958 (CH), 2872 (CH), 1740 (C=O), 1670 (C=C) cm^{-1}. ^1H NMR (400 MHz, $CDCl_3$): δ 0.80 (d, J = 6.8 Hz, 6 H, C(O)CH$_2$CH(CH*Me*$_2$)$_2$), 0.89 (d, J = 6.8 Hz, 6 H, C(O)CH$_2$CH(CH*Me*$_2$)$_2$), 0.93 (d, J = 6.6 Hz, 6 H, C=CHCH$_2$CH*Me*$_2$), 1.58 (app pentet, 1 H, C=CHCH$_2$C*H*Me$_2$), 1.67−1.77 (m, 3 H, C(O)CH$_2$*CH*(C*H*Me$_2$)$_2$), 2.19 (d, J = 5.7 Hz, 2H, C(O)C*H*$_2$CH(CHMe$_2$)$_2$), 2.38 (t, J = 6.8 Hz, 1H, CH$_2$O*H*), 2.59−2.63 (m, 2 H, C=CHC*H*$_2$-CHMe$_2$), 2.69−2.75 (overlapping dtd, J_{gem} = 16.6 Hz, 1 H, lactone-C*H*$_2$), 2.88−2.94 (overlapping dtd, J_{gem} = 16.4 Hz, 1 H, lactone-C*H*$_2$), 3.62 (dd, J = 12.1, 6.6 Hz, 1 H, C*H*$_2$OH), 3.70 (dd, J = 12.2, 7.0 Hz, 1 H, C*H*$_2$OH), 4.19 (AB quartet, J = 11.9 Hz, 2 H, C*H*$_2$OC(O)CH$_2$CH(CHMe$_2$)$_2$), 6.26 (tt, J = 7.8, 2.3 Hz, 1H, C = *CH*CH$_2$CHMe$_2$). ^{13}C NMR (100 MHz, $CDCl_3$): δ 18.67, 21.30, 22.26, 22.28, 28.59, 29.34, 32.75, 39.10, 36.32, 46.84, 64.66, 65.34, 82.30, 124.47, 144.42, 168.68, 174.72. FAB-MS (*m*/*z*, relative intensity): 355 (MH^+, 47). Anal. ($C_{20}H_{34}O_5$) C, H.

(*E*)-[2-(Hydroxymethyl)-4-(3-methylbutylidene)-5-oxo-2-2,3-dihydrofuryl]methyl-4-methyl-3-(methylethyl)pentanoate (7*E*). Yield: 0.045 g, 54%, white solid; mp 32−33 °C. IR (neat): 3462 (OH), 2958 (CH), 2873 (CH), 1741 (C=O), 1681 (C=C) cm^{-1}. ^1H NMR (400 MHz, $CDCl_3$): δ 0.79 (dd, J = 6.7, 1.1 Hz, 6 H, C(O)CH$_2$CH(CH*Me*$_2$)$_2$), 0.88 (d, J = 6.8 Hz, 6 H, C(O)CH$_2$CH(CH*Me*$_2$)$_2$), 0.94 (d, J = 6.6 Hz, 6 H, C=CHCH$_2$-CH*Me*$_2$), 1.54−1.60 (m, 1 H, C(O)CH$_2$C*H*(CHMe$_2$)$_2$), 1.68−1.86 (m, 3 H, C=CHCH$_2$C*H*Me$_2$ and C(O)CH$_2$CH(C*H*Me$_2$)$_2$), 2.04−2.08 (m, 2 H, C=CHC*H*$_2$CHMe$_2$), 2.18 (d, J = 5.9 Hz, 2 H, C(O)C*H*$_2$CH(CHMe$_2$)$_2$), 2.50 (t, J = 6.4 Hz, 1H, CH$_2$O*H*), 2.62−2.68 (overlapping dtd, J_{gem} = 17.0 Hz, 1 H, lactone-C*H*$_2$), 2.79−2.85 (overlapping dtd, J_{gem} = 17.2 Hz, 1 H, lactone-C*H*$_2$), 3.64 (dd, J = 12.1, 6.4 Hz, 1 H, C*H*$_2$OH), 3.72 (dd, J = 12.2, 6.7 Hz, 1 H, C*H*$_2$OH), 4.20 (AB quartet, J = 11.9 Hz, 2 H, C*H*$_2$OC-(O)CH$_2$CH(CHMe$_2$)$_2$), 6.76−6.81 (m, 1H, C = *CH*CH$_2$CHMe$_2$). ^{13}C NMR (100 MHz, $CDCl_3$): δ 18.67, 21.29, 21.30, 22.40, 28.09, 29.33, 29.34, 29.91, 32.74, 39.31, 46.85, 64.81, 65.48, 83.07, 126.62, 140.83, 169.87, 174.68. FAB-MS (*m*/*z*, relative intensity): 355 (MH^+, 93), 57 (100). Anal. ($C_{20}H_{34}O_5$) C, H.

(*Z*)-{2-(Hydroxymethyl)-4-[4-methyl-3-(methylethyl)-pentylidene]-5-oxo-2-2,3-dihydrofuryl}methyl-3-methylbutanoate (9*Z*). Under argon, Bu_2SnO (0.075 g, 0.30 mmol) was added to a solution of **19*Z*** (0.054 g, 0.20 mmol) in PhMe (5.0 mL) containing 4 Å molecular sieves and heated to reflux. After 3 h, the reaction was cooled to 0 °C, isovaleryl chloride (27 μL) was added, and the reaction was allowed to warm to room temperature overnight. The reaction mixture was then quenched with pH 7 buffer solution, extracted with $CHCl_3$ (3×), dried over $MgSO_4$, and concentrated. Purification by silica gel chromatography gave **9*Z*** as a colorless oil (0.013 g, 18%). IR (neat): 3545 (OH), 2958 (CH), 2927 (CH), 1737 (C=O), 1671 (C=C) cm^{-1}. ^1H NMR (400 MHz, $CDCl_3$): δ 0.83 (dd, J = 6.7, 1.5 Hz, 6 H, C=CHCH$_2$CH(CH*Me*$_2$)$_2$), 0.87 (dd, J = 6.8, 1.4 Hz, 6 H, C=CHCH$_2$CH(CH*Me*$_2$)$_2$), 0.92 (d, J = 6.6 Hz, 6 H, C(O)CH$_2$CH*Me*$_2$), 1.08 (pentet, J = 5.5 Hz, 1 H, C=CHCH$_2$C*H*(CHMe$_2$)$_2$), 1.69−1.80 (m, 2 H, C=CHCH$_2$CH-(C*H*Me$_2$)$_2$), 2.00−2.10 (m, 1 H, C(O)CH$_2$C*H*Me$_2$), 2.18 (d, J = 6.8 Hz, 2 H, C(O)C*H*$_2$CHMe$_2$), 2.64−2.71 (m, 3 H, C=CHC*H*$_2$-CH(CHMe$_2$)$_2$ and lactone-C*H*$_2$), 2.82−2.88 (m, 1 H, lactone-C*H*$_2$), 3.62 (AB quartet, J = 12.2 Hz, 2 H, C*H*$_2$OH), 4.18 (AB quartet, J = 11.9 Hz, 2 H, *CH*$_2$OC(O)CH$_2$CHMe$_2$), 6.20−6.26 (m, 1H, C = *CH*CH$_2$CH(CHMe$_2$)$_2$). ^{13}C NMR (100 MHz, $CDCl_3$): δ 19.61, 21.82, 22.54, 25.80, 26.53, 29.54, 33.41, 43.27, 51.39, 64.89, 65.29, 82.37, 112.81, 148.08, 168.62, 173.12. FAB-MS (*m*/*z*, relative intensity): 355 (MH^+, 100). Anal. ($C_{20}H_{34}O_5$) C, H.

(*E*)-{2-(Hydroxymethyl)-4-[4-methyl-3-(methylethyl)-pentylidene]-5-oxo-2-2,3-dihydrofuryl}methyl-3-methylbutanoate (9*E*). Under argon, Bu_2SnO (0.433 g, 1.7 mmol) was added to a solution of **19*E*** (0.314 g, 1.2 mmol) in PhMe (20 mL) containing 4 Å molecular sieves and heated to reflux. After 2 h, the reaction was cooled to 0 °C, isovaleryl chloride

(156 μL) was added, and the reaction was allowed to warm to room temperature over the weekend. The reaction mixture was then quenched with pH 7 buffer solution, extracted with $CHCl_3$ (3×), dried over $MgSO_4$, and concentrated. Purification by silica gel chromatography gave **9***E* as a colorless oil (0.085 g, 21%). IR (neat): 3447 (OH), 2958 (CH), 2873 (CH), 1740 (C=O), 1676 (C=C) cm^{-1}. ^1H NMR (400 MHz, $CDCl_3$): δ 0.81 (d, J = 6.9 Hz, 6 H, C=CHCH$_2$CH(CHMe_2)$_2$), 0.87 (dd, J = 6.9, 0.9 Hz, 6 H, C=CHCH$_2$CH(CHMe_2)$_2$), 0.91 (d, J = 6.5 Hz, 6 H, C(O)CH$_2$CHMe_2), 1.14−1.21 (m, 1 H, C=CHCH$_2$C*H*-(CHMe$_2$)$_2$), 1.70−1.79 (m, 2 H, C=CHCH$_2$CH(C*H*Me$_2$)$_2$), 1.97−2.11 (m, containing 1 H, C(O)CH$_2$C*H*Me$_2$ and 2 H, C=CHCH_2CH(CHMe$_2$)$_2$), 2.17 (d, J = 0.9 Hz, 2 H, C(O)CH_2CHMe$_2$), 2.60−2.66 (overlapping dtd, J_{gem} = 17.0 Hz, 1 H, lactone-CH_2), 2.76−2.82 (overlapping dtd, J_{gem} = 17.1 Hz, 1 H, lactone-CH_2), 3.65 (AB quartet, J = 12.2 Hz, 2 H, CH_2OH), 4.19 (AB quartet, J = 11.9 Hz, 2 H, CH_2OC(O)CH$_2$CHMe$_2$), 6.75−6.80 (m, 1H, C = *C*HCH$_2$CH(CHMe$_2$)$_2$). ^{13}C NMR (100 MHz, $CDCl_3$): δ 19.49, 19.54, 21.76, 21.82, 22.53, 25.79, 28.90, 29.40, 30.15, 43.24, 50.51, 65.01, 65.48, 83.20, 125.04, 144.17, 170.19, 173.05. FAB-MS (*m*/*z*, relative intensity): 355 (MH^+, 100). Anal. ($C_{18}H_{30}O_5 \cdot 0.5H_2O$) C, H.

References

(1) Newton, A. C. Protein Kinase C: Structure, Function and Regulation. *J. Biol. Chem*. **1995**, *270*, 28495−28498.

(2) Quest, A. F. G. Regulation of protein kinase C: A tale of lipids and proteins. *Enzyme Protein* **1996**, *49*, 231−261.

(3) Mellor, H.; Parker, P. J. The extended protein kinase C superfamily. *Biochem. J*. **1998**, *332*, 281−292.

(4) Ron, D.; Kazanietz, M. G. New insights into the regulation of protein kinase C. and novel phorbol ester receptors. *FASEB J*. **2000**, *13*, 1658−1676.

(5) Castagna, M.; Takai, Y.; Kaibuchi, K.; Sano, K.; Kikkawa, U.; Nishizuka, Y. Direct activation of calcium-activated, phospholipid-dependent protein kinase by tumor-promoting phorbol esters. *J. Biol. Chem*., **1982**, *257*, 7847−7851.

(6) Newton, A. C. Protein Kinase C: Structural and spatial regulation by phosphorylation, cofactors, and macromolecular interactions. *Chem. Rev*., **2001**, *101*, 2353−2364.

(7) Sakai, N.; Sadaki, K.; Ikegaki, N.; Shirai, Y.; Ono, Y.; Saito, N. Direct visualization of the translocation of the γ-subspecies of protein kinase C in living cells using fusion proteins with green fluorescent protein. *J. Cell Biol*. **1997**, *139*, 1465−1476.

(8) Oancea, E.; Teruel, M. N.; Quest, A. F. G.; Meyer, T. Green fluorescent protein (GFP)-tagged cysteine-rich domains from protein kinase C as fluorescent indicators for diacylgylcerol signaling in living cells. *J. Cell Biol*. **1998**, *140*, 485−498.

(9) Newton, A. C.; Keranen, L. M. Phosphatidyl-L-serine is necessary for protein kinase C's high affinity interaction with diacylglycerol-containing membranes. *Biochemistry* **1994**, *33*, 661−6658.

(10) Newton, A. C. Regulation of protein kinase C. *Curr. Opin. Cell. Biol*. **1997**, *9*, 161−167.

(11) Nishizuka, Y. Intracelluar signaling by hydrolysis of phospholipids and activation of protein-kinase-C. *Science* **1992**, *258*, 607−614.

(12) Oancea, E.; Meyer, T. Protein kinase C as a molecular machine for decoding calcium and diacylglycerol signals. *Cell* **1998**, *95*, 307−318.

(13) Zhang, G. G.; Kazanietz, M. G.; Blumberg, P. M.; Hurley, J. H. Crystal structure of the cys2 activator-binding domain of protein kinase C delta in complex with phorbol ester. *Cell* **1995**, *81*, 917−924.

(14) Nacro, K.; Bienfait, B.; Lewin, N. E.; Blumberg, P. M.; Marquez, V. E. Diacylglycerols with lipophilically equivalent branched acyl chains display high affinity for protein kinase C (PK-C). A direct measure of the effect of constraining the glycerol backbone in DAG lactones. *Bioorg. Med. Chem. Lett*. **2000**, *10*, 653−655.

(15) Nacro, K.; Bienfait, B.; Lee, J.; Han, K.-C.; Kang, J.-H.; Benzaria, S.; Lewin, N. E.; Bhattacharyya, D. K.; Blumberg, P. M.; Marquez, V. E. Confromationally Constrained Analogues of Diacylglycerol (DAG). 16. How Much Structural Complexity is Necessary for Recognition and High Binding Affinity to Protein Kinase C? *J. Med. Chem*. **2000**, *43*, 921−944.

(16) Nacro, K.; Sigano, D. M.; Yan, S.; Nicklaus, M.; Pearce, L. L.; Lewin, N. E.; Garfield, S. H.; Blumberg, P. M.; Marquez, V. E. An optimized protein Kinase C Activating Diacylglycerol Combining High Binding Affinity (Ki) with Reduced Lipophilicity (log P). *J. Med. Chem*. **2001**, *44*, 1892−1904.

(17) For compound **6**: Hanessian, S.; Abad-Grillo, T.; McNaughton-Smith, G. Synthesis of (4*S*)-hydroxymethyl-(2*R*)-(2-propyl)butyrolactone: a quest for a practical route to an important hydroxyethylene isostere chiron. *Tetrahedron* **1997**, *53*, 6281−6294.

(18) Sharma, R.; Lee, J.; Wang, S.; Milne, G. W. A.; Lewin, N. E.; Blumberg, P. M.; Marquez, V. E. Conformationally Constrained Analogues of Diacylglycerol.10. Ultrapotent Protein Kinase C Ligands Based on a Racemic 5-Disubstituted Tetrahydro-2-furanone Template. *J. Med. Chem*. **1996**, *39*, 19−28.

(19) Bögi, K.; Lorenzo, P. S.; Àcs, P.; Szállási, Z.; Wagner, G. S.; Blumberg, P. M. Comparison of the roles of the C1a and C1b domains of protein kinase C alpha in ligand induced translocation in NIH 3T3 cells. *FEBS Lett*. **1999**, *456*, 27−30.

(20) Meylan, W. M.; Howard, Ph. H. Atom Fragment Contribution Method for Estimating Octanol−Water Partition Coefficients. KOWWIN 1.63, Syracuse Research Corp.; http://esc.syrres.com.20. *J. Pharm. Sci*. **1995**, *84*, 83−92.

(21) Lee, J.; Shaomeng Wang, S.; Milne, G. W. A.; Sharma, R.; Lewin, N. E.; Blumberg, P. M.; Marquez, V. E. Conformationally Constrained Analogues of Diacylglycerol. 11.1 Ultrapotent Protein Kinase C Ligands Based on a Chiral 5-Disubstituted Tetrahydro-2-furanone Template. *J. Med. Chem*. **1996**, *39*, 29−35.

(22) Rarey, M.; Kramer, B.; Lengauer, T.; Klebe, G. A fast flexible docking method using an incremental construction algorithm. *J. Mol. Biol*. **1996**, *261*, 470−489.

(23) Jones, G.; Willett, P.; Glen, R. C. Molecular recognition of receptor sites using a genetic algorithm with a description of desolvation. *J. Mol. Biol*. **1995**, *245*, 43−53.

(24) Benzaria, S.; Bienfait, B.; Nacro, K.; Wang, S.; Lewin, N. E.; Beheshti, M.; Blumberg, P. M.; Marquez, V. E. Conformationally constrained analogues of diacylglycerol (DAG). 15. The indispensable role of the *sn*-1 and *sn*-2 carbonyls in the binding of DAG-lactones to protein kinase C (PK-C). *Bioorg. Med. Chem. Lett*. **1998**, *8*, 3403−3408.

(25) Numbering of the PK-C residues is internal to the C1 domain (e.g., Gly 23 corresponds to Gly 253 in PK-Cδ C1b, Gly 59 in PK-Cα C1a, and Gly 124 in PK-Cα C1b).

(26) Insight II and QUANTA 97 are products of Accelrys Inc., 9685 Scranton Road, San Diego, CA 92121-3752 (www.accelrys.com).

(27) Bower, M.; Cohen, F. E.; Dunbrack, R. L., Jr. Side chain placement from a backbone-dependent rotamer library: A new tool for homology modeling. *J. Mol. Biol*. **1997**, *267*, 1268−1282.

(28) FlexX and SYBYL are products of Tripos Inc., 1699 South Hanley Road, St. Louis, MO 63144-2913 (www.tripos.com).

(29) Brooks, B. R.; Bruccoleri, R. E.; Olafson, B. D.; States, D. J.; Swaminnathan, S.; Karplus, M. CHARMM: A program for macromolecular energy, minimization, and dynamics calculations. *J. Comput. Chem*. **1983**, *4*, 187−217.

(30) Momany, F. A.; Rone, R. Validation of the general purpose QUANTA 3.2/CHARMm force field. *J. Comput. Chem*. **1992**, *13*, 888−900.

(31) Lee, B.; Richards, F. M. The interpretation of protein structures: Estimation of static accessibility. *J. Mol. Biol*. **1971**, *55*, 379−400.

JM020476O